A transcriptional network underlying migratory cellular states and reduced 5-ALA-based photodynamic detectability in glioblastoma

WENYU LIU[1*], TINGTING ZHANG[1*], ICHIYO SHIBAHARA[2], TAKUICHIRO HIDE[2], TOSHIHIRO KUMABE[2], SHUN-ICHIRO OGURA[3], TETSUYA TAGA[1] and KOUICHI TABU[1,4]

[1]Department of Stem Cell Regulation, Division of Visionary Life Science, Medical Research Laboratory, Institute of Integrated Research, Institute of Science Tokyo, Tokyo 113-8510, Japan; [2]Department of Neurosurgery, Kitasato University School of Medicine, Sagamihara, Kanagawa 252-0374, Japan; [3]School of Life Science and Technology, Institute of Science Tokyo, Yokohama, Kanagawa 226-8501, Japan

Received November 22, 2025; Accepted March 10, 2026

DOI: 10.3892/mco.2026.2958

Abstract. Surgical resection remains the cornerstone of the standard therapy for glioblastoma (GBM), yet postoperative recurrence remains a major clinical challenge. Intraoperative photodynamic detection (PDD) using 5-aminolevulinic acid (5-ALA) improves the precision of tumor removal. However, a subset of tumor cells can evade fluorescence-based detection, potentially contributing to residual disease and relapse. The present study analyzed the relationship between cellular migratory capacity and 5-ALA PDD visibility using six patient-derived GBM cell lines (KBT#12137, KBT#10135, KBT#10170, PDM19, PDM22 and PDM123). This study revealed a positive correlation, indicating that cells with higher migratory potential accumulated lower levels of 5-ALA-induced protoporphyrin IX and were therefore more likely to escape intraoperative detection. Transcriptomic profiling identified gene expression signatures specifically associated with this phenotype, highlighting pathways related to cytoskeletal regulation, heme metabolism, and transporter activity. These findings suggest that the migratory potential and diagnostic evasion are functionally linked through shared molecular programs, thereby providing a potential basis for identifying predictive biomarkers associated with incomplete resection and recurrence risk. Overall, this study provides insights that may contribute to improved intraoperative strategies and targeted therapeutic approaches for GBM.

Correspondence to: Dr Kouichi Tabu, Department of Stem Cell Regulation, Division of Visionary Life Science, Medical Research Laboratory, Institute of Integrated Research, Institute of Science Tokyo, 1-5-45 Yushima, Bunkyo-ku, Tokyo 113-8510, Japan
E-mail: k-tabu.scr@mri.tmd.ac.jp

[4]*Present address:* Department of Robotic Science, Division of Biological Data Science, Medical Research Laboratory, Institute of Integrated Research, Institute of Science Tokyo, 1-5-45 Yushima, Bunkyo-ku, Tokyo 113-8510, Japan

[*]Contributed equally

Abbreviations: GBM, glioblastoma; 5-ALA, 5-aminolevulinic acid; PpIX, protoporphyrin IX; FGS, fluorescence-guided surgery; DEG, differentially expressed gene; FDR, false discovery rate

Key words: glioblastoma, photodynamic detection, 5-aminolevulinic acid, protoporphyrin IX, intraoperative fluorescence, cell migration, transcriptomics, cancer stem cells

Introduction

Glioblastoma (GBM) is an aggressive primary brain tumor characterized by diffuse infiltration and inevitable recurrence, despite multimodal therapy comprising surgical resection, radiotherapy, and temozolomide chemotherapy (1,2). The extent of resection is among the strongest prognostic factors for GBM. However, achieving maximal and safe resection is technically challenging because tumor cells often extend beyond radiographically apparent margins and intermingle with eloquent brain tissue (3-7).

To enhance intraoperative visualization of tumor tissue, photodynamic detection (PDD) with 5-aminolevulinic acid (5-ALA) has been widely adopted (8-10). Following systemic administration, 5-ALA is metabolized to protoporphyrin IX (PpIX), which preferentially accumulates in many GBM cells and emits red fluorescence under violet-blue excitation, thus enabling real-time guidance for resection (8,11,12). Randomized and observational studies have demonstrated that 5-ALA-guided surgery increases the rate of complete resection and improves short-term outcomes compared to white-light resection alone (11,13). Nevertheless, fluorescence-negative tumor foci do occur, and residual disease is frequently found in peritumoral and infiltrative regions, even after PDD-assisted resections, underscoring the biological heterogeneity in PpIX accumulation and diagnostic evasion during surgery (14-17).

Among the potential determinants of PDD visibility, two biological features may be relevant to surgical failure: i) cellular motility or migration, which drives dissemination along white matter tracts and vascular niches, leading to non-contiguous

microscopic disease; and ii) metabolic programs controlling PpIX biosynthesis, export, and degradation, which modulate the fluorescence yield upon 5-ALA exposure (18-21). Previous studies suggested that subpopulations with stem-like or stress-adapted traits exhibit altered porphyrin metabolism and reduced PpIX fluorescence, potentially facilitating escape from intraoperative detection and subsequent persistence after resection (12,14,22). However, whether the migratory capacity and PDD visibility are coupled at the level of shared molecular programs has not yet been systematically evaluated using patient-derived GBM models.

Glioblastoma progression and spatial dissemination are critically shaped by the tumor microenvironment, which provides structural, metabolic, and paracrine support for tumor cell migration and survival (23-26). Hypoxic gradients, perivascular niches, extracellular matrix remodeling, and cytokine-mediated signaling have been shown to promote mesenchymal-like transcriptional programs associated with enhanced motility, metabolic plasticity, and therapeutic resistance (23-25,27). Although GBM arises from non-epithelial tissue, tumor cells frequently acquire migration-associated cellular states that share features with epithelial-mesenchymal transition, including cytoskeletal reorganization and altered adhesion dynamics, without undergoing classical epithelial marker conversion (27,28). These findings indicate that the migratory capacity reflects the integration of microenvironmental signals into coordinated transcriptional programs that support tumor progression and dissemination.

Here, using six patient-derived GBM cell lines (KBT#12137, KBT#10135, KBT#10170, PDM19, PDM22, and PDM123), we quantitatively assessed cellular migratory capacity and 5-ALA-induced PpIX accumulation and tested their relationship. We performed transcriptomic profiling to identify the gene expression signatures associated with the combined phenotype. Our analyses revealed a positive correlation, indicating that cells with higher migratory potential displayed lower PpIX accumulation and, therefore, reduced PDD visibility. Transcriptome-wide comparisons highlighted the enrichment of pathways related to cytoskeletal regulation, heme/porphyrin metabolism, and transporter activity associated with this phenotype.

Collectively, these findings support a functional link between migratory capacity and intraoperative diagnostic evasion of GBM. From a translational perspective, the results identify candidate molecular markers that may predict incomplete resection and recurrence risk and suggest testable strategies to enhance PDD visibility, such as modulation of heme biosynthesis and transport, or to combine PDD-guided resection with adjunctive photodynamic therapy in molecularly defined settings (29,30). This study provides a compact and mechanistically informed foundation for future validation and intervention studies.

Materials and methods

Patient-derived GBM cell culture and reagents. Six patient-derived glioblastoma (GBM) cell lines (KBT#12137, KBT#10135, KBT#10170, PDM19, PDM22, and PDM123) were kindly provided by Dr. Takuichiro Hide (Department of Neurosurgery, Kitasato University School of Medicine, Kanagawa, Japan). All cell lines were established from primary GBM tissues using protocols approved by the Institutional Ethics Committee, and informed consent was obtained from all patients prior to tissue collection.

Primary GBM tissues obtained by surgical resection were mechanically minced and enzymatically dissociated into single-cell suspensions. The cell suspensions were filtered through a 70-μm cell strainer to remove debris and plated under serum-free conditions to promote sphere formation. Under these conditions, the cells formed free-floating neurospheres with a spherical morphology and well-defined borders, consistent with previously described patient-derived GBM neurosphere cultures.

Cells were maintained as neurospheres in serum-free Dulbecco's modified Eagle's medium/Nutrient Mixture F-12 (DMEM/F12; Gibco, Massachusetts, USA; Cat. No. 21331020) supplemented with 20 ng/ml human epidermal growth factor (EGF; PeproTech, USA; Cat. No. AF-100-15-500UG), 20 ng/ml human basic fibroblast growth factor (bFGF; Oriental Yeast Co., Ltd., Japan; Cat. No. 47079000), 20 ng/ml leukemia inhibitory factor (LIF; Oriental Yeast; Cat. No. 47076000), 0.5x N2 supplement (Thermo Fisher Scientific, USA; Cat. No. 17502048), 0.5x B27 supplement (Thermo Fisher Scientific; Cat. No. 17504044), 1x GlutaMAX (Thermo Fisher Scientific; Cat. No. 35050061), 1x penicillin-streptomycin (Thermo Fisher Scientific; Cat. No. 15140122), 5 μg/ml heparin (Sigma-Aldrich, Japan; Cat. No. H3149-10KU), and 10 ng/ml insulin (Sigma-Aldrich, Japan; Cat. No. I6634-50MG). Cultures were incubated in a humidified atmosphere with 5% CO_2 at 37˚C and passaged every 7-10 days by gentle mechanical dissociation. The 5-aminolevulinic acid (5-ALA) hydrochloride was purchased from Cosmo Oil Co., Ltd. (Tokyo, Japan; Cat. No. AL-00-1).

Detection of PpIX fluorescence by flow cytometry and microscopy. To assess the cellular accumulation of PpIX following 5-ALA exposure, patient-derived cells were dissociated into single cells and seeded at a density of $5x10^4$ cells/ml. The cells were then incubated with 1 mM of 5-ALA for 4 h at 37˚C under 5% CO_2. After incubation, PpIX fluorescence was analyzed by flow cytometry (FACS Aria II, BD Biosciences, USA). Fluorescence was excited with a 488-nm laser and detected using a 660/20-nm band-pass filter. The data were processed using FlowJo software (v7.6.5; TOMY Digital Biology, Japan).

For microscopic observation, PpIX fluorescence was visualized using a fluorescence microscope (Bio-Revo BZ-9000, Keyence, Japan) equipped with a QD625 filter cube (Olympus, Japan). At least three independent experiments were performed for each condition, and representative results are shown.

Transwell migration assay for selection of migratory and non-migratory populations. Cell motility was evaluated using 24-well Transwell chambers with 8-μm pore polycarbonate membranes (Corning, #3422). Single-cell suspensions ($2x10^5$ cells/100 μl) in serum-free DMEM/F12 were placed into the upper chamber, and 600 μl of complete sphere medium was added to the lower chamber as a chemoattractant. After 72 h incubation at 37˚C, non-migratory cells remaining on the upper surface were collected by gentle trypsinization,

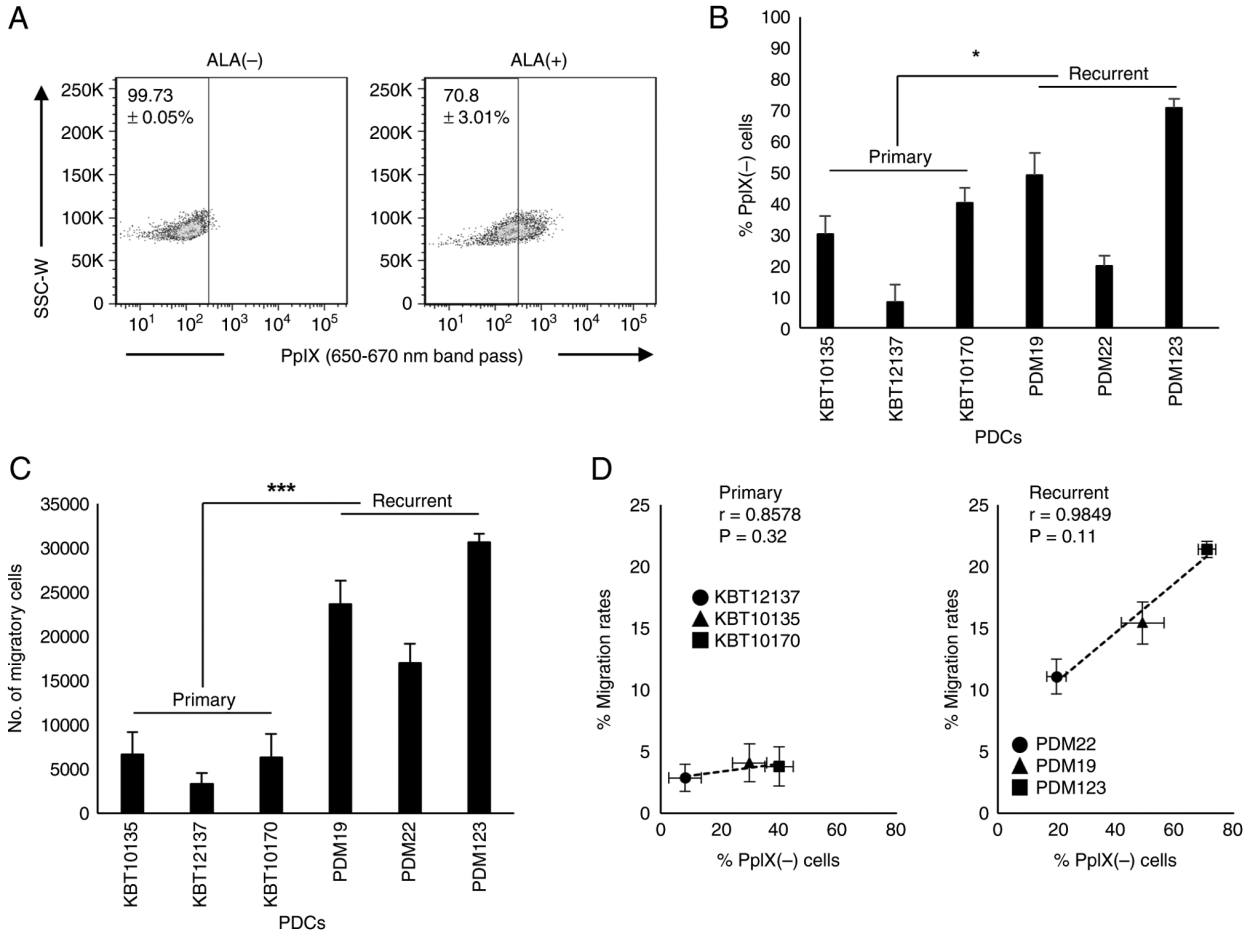

Figure 1. Correlation between PpIX accumulation and migratory potential in patient-derived GBM cells. (A) Representative flow cytometry histograms showing 5-ALA-induced PpIX fluorescence in the recurrent GBM line PDM123. (B) Quantification of PpIX-negative cell fractions in three primary (KBT series) and three recurrent (PDM series) GBM lines. KBT#12137 showed the highest PpIX accumulation, whereas PDM123 exhibited the lowest, consistent with its recurrent origin. Significant differences were observed between the primary and recurrent groups. *P<0.05. (C) Quantitative analysis of migratory capacity assessed by Transwell assay across the six GBM lines. Recurrent lines displayed significantly higher motility than primary lines. ***P<0.001. (D) Correlation between the proportion (%) of PpIX-negative cells and the migratory index, defined as the migration rate (%)=(lower-/upper-chamber cell counts) x100. All data represent means ± SD from at least three independent experiments. GBM, glioblastoma; 5-ALA, 5-aminolevulinic acid; PpIX, protoporphyrin IX.

while migratory cells that had traversed the membrane were recovered from the lower chamber.

To ensure reproducibility, migration assays were performed in triplicate using independent cell preparations. Both fractions were treated with 5-ALA, as described above, to assess the relationship between migratory capacity and PpIX accumulation. The combination of migration status (migratory vs. non-migratory) and fluorescence phenotype ($PpIX^+$ vs. $PpIX^-$) yielded four distinct subpopulations, which were used for downstream transcriptomic analysis.

RNA extraction and cDNA microarray analysis. Total RNA was extracted from the four subpopulations described above (migratory $PpIX^+$, migratory $PpIX^-$, non-migratory $PpIX^+$, and non-migratory $PpIX^-$) using the RNeasy Plus Micro Kit (Qiagen, #74034) according to the manufacturer's protocol. RNA integrity was assessed using a Bioanalyzer (Agilent Technologies), and only samples with an RNA integrity number (RIN) >9.0 were used. For transcriptome profiling, genome-wide cDNA microarray analysis was outsourced to the Chemicals Evaluation and Research Institute (CERI, Tokyo, Japan) and performed using the Agilent Human Whole Genome Oligo Microarray platform (4x44 K, G4112F). Differentially expressed genes (DEGs) were defined as those showing a fold-change greater than 2 and a false discovery rate (FDR) <0.05. Data normalization and statistical analyses were conducted using the GeneSpring GX software (Agilent Technologies).

Gene set enrichment analysis (GSEA). To elucidate biological pathways associated with PpIX detection resistance and cell motility, DEGs identified in microarray data were subjected to GSEA (31). Analyses were performed using the fgsea R package (v1.26.0; Bioconductor) with Molecular Signatures Database Hallmark and Gene Ontology gene sets (32,33). Genes were ranked according to the $\log_2$ fold change between groups, and enrichment scores were calculated using 10,000 permutations. Significantly enriched pathways were defined by a FDR<0.05. Functional categories related to cytoskeleton regulation, heme metabolism, and membrane transport are highlighted.

The Cancer Genome Atlas (TCGA) data analysis. Public transcriptomic data of patients with GBM (n=525) were obtained

from TCGA (TCGA_GBM; HG-U133A platform) using the GlioVis portal (https://gliovis.bioinfo.cnio.es/) (34).

Statistical analysis. All data are expressed as the mean ± standard deviation (SD). Comparisons between two groups were performed using unpaired two-tailed Student's t-test, and correlations were analyzed using Pearson's correlation coefficient. Survival differences in TCGA data were evaluated using Kaplan-Meier survival analysis with log-rank and Gehan-Breslow-Wilcoxon tests. A P-value <0.05 was considered to indicate a statistically significant difference.

Results

Migratory capacity inversely correlates with 5-ALA-induced PpIX accumulation in patient-derived GBM cells. To assess whether migratory potential influences intraoperative detectability in GBM, we examined the relationship between cell motility and 5-ALA-induced PpIX fluorescence in six patient-derived GBM cell lines (KBT#10135, KBT#12137, KBT#10170, PDM19, PDM22, and PDM123). Flow cytometric analysis of the recurrent GBM cell line PDM123 revealed heterogeneous PpIX fluorescence with a distinct population lacking detectable signals (Fig. 1A). Across the six lines, the proportion of PpIX-negative cells varied substantially, with the primary line KBT#12137 showing the highest PpIX accumulation and the recurrent line PDM123 showing the lowest (approximately 70% PpIX-negative cells) (Fig. 1A and B). Although the recurrent lines tended to exhibit weaker fluorescence than the primary lines, the difference between the two groups was statistically significant (P<0.05; two-tailed t-test, n=3 lines per group). Transwell migration assays demonstrated that recurrent GBM cell lines exhibited significantly higher migratory activity than primary cell lines (P<0.05; two-tailed t-test, n=3 lines per group) (Fig. 1C). When the proportion of PpIX-negative cells was plotted against the migratory index [defined as the migration rate (%)=(lower-/upper-chamber cell counts) x100], positive correlations were observed within both the primary and recurrent groups (Pearson's r=0.8578 and 0.9849, respectively; Fig. 1D). The overall correlation across all six lines was positive (Pearson's r=0.7852). These findings demonstrate that highly motile GBM cells accumulate lower levels of PpIX upon 5-ALA exposure and are thus less detectable during fluorescence-guided surgery. Collectively, these data support functional coupling between intrinsic motility and diagnostic invisibility, which may contribute to incomplete tumor removal and postsurgical recurrence.

Highly migratory GBM cells exhibit reduced 5-ALA detectability. To further test whether the migration status directly affects 5-ALA detectability at the subpopulation level, each patient-derived GBM culture was fractionated into migratory and non-migratory populations using Transwell assays, followed by PpIX fluorescence analysis. In the recurrent line PDM123, the migratory (lower chamber) population contained a markedly higher proportion of PpIX-negative cells than the non-migratory (upper chamber) population (Fig. 2A). This trend was consistently observed across all six GBM cell lines, with five lines (all except PDM19) showing a significantly greater proportion of PpIX-negative cells in the migratory

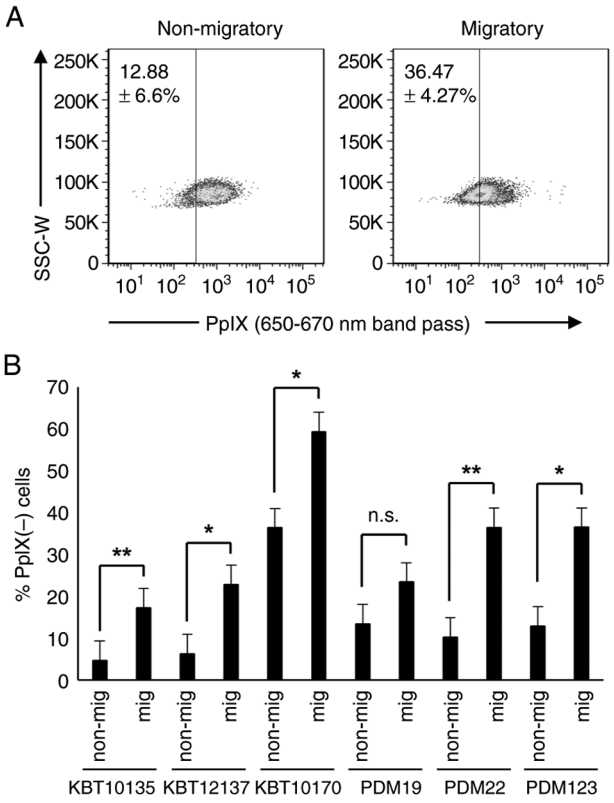

Figure 2. Reduced PpIX accumulation in highly migratory GBM subpopulations. (A) Representative comparison of 5-ALA-induced PpIX fluorescence between migratory (lower-chamber) and non-migratory (upper-chamber) cells isolated from the recurrent GBM line PDM123. The migratory fraction contained a higher proportion of PpIX-negative cells. (B) Quantitative summary of PpIX-negative cell fractions in migratory and non-migratory subpopulations across six GBM lines (three primary and three recurrent). Except for PDM19, all lines exhibited a significantly higher frequency of PpIX-negative cells in the migratory fraction. *P<0.05 and **P<0.01. Data represent means ± SD from at least three independent experiments. GBM, glioblastoma; 5-ALA, 5-aminolevulinic acid; PpIX, protoporphyrin IX; n.s., not significant.

fraction (*P<0.05, **P<0.01) (Fig. 2B). The relative abundance of the migratory PpIX-negative population was positively correlated with the overall migratory index across cell lines (r=0.72, P<0.05). Thus, 5-ALA detectability is inversely linked to migratory behavior and a minor subpopulation that combines high motility with low fluorescence likely represents a surgically invisible fraction that contributes to tumor infiltration and recurrence.

Transcriptomic and clinical characterization of the migratory PpIX-low phenotype. To define the molecular programs underlying this dual phenotype, we performed genome-wide transcriptomic profiling of four phenotypically defined subpopulations-migratory PpIX-high, migratory PpIX-low, non-migratory PpIX-high, and non-migratory PpIX-low-sorted from representative GBM lines. Genes specifically upregulated in the migratory PpIX-low subset were defined by combined criteria of selectivity and amplitude ($\log_2$FC_rest >1 and $\log_2$FC_CA, CB, CD >0.5). Under this definition, migratory PpIX-low cells exhibited a focused but distinct transcriptional signature comprising 10 upregulated and 42 downregulated genes, relative to the other three groups. The upregulated

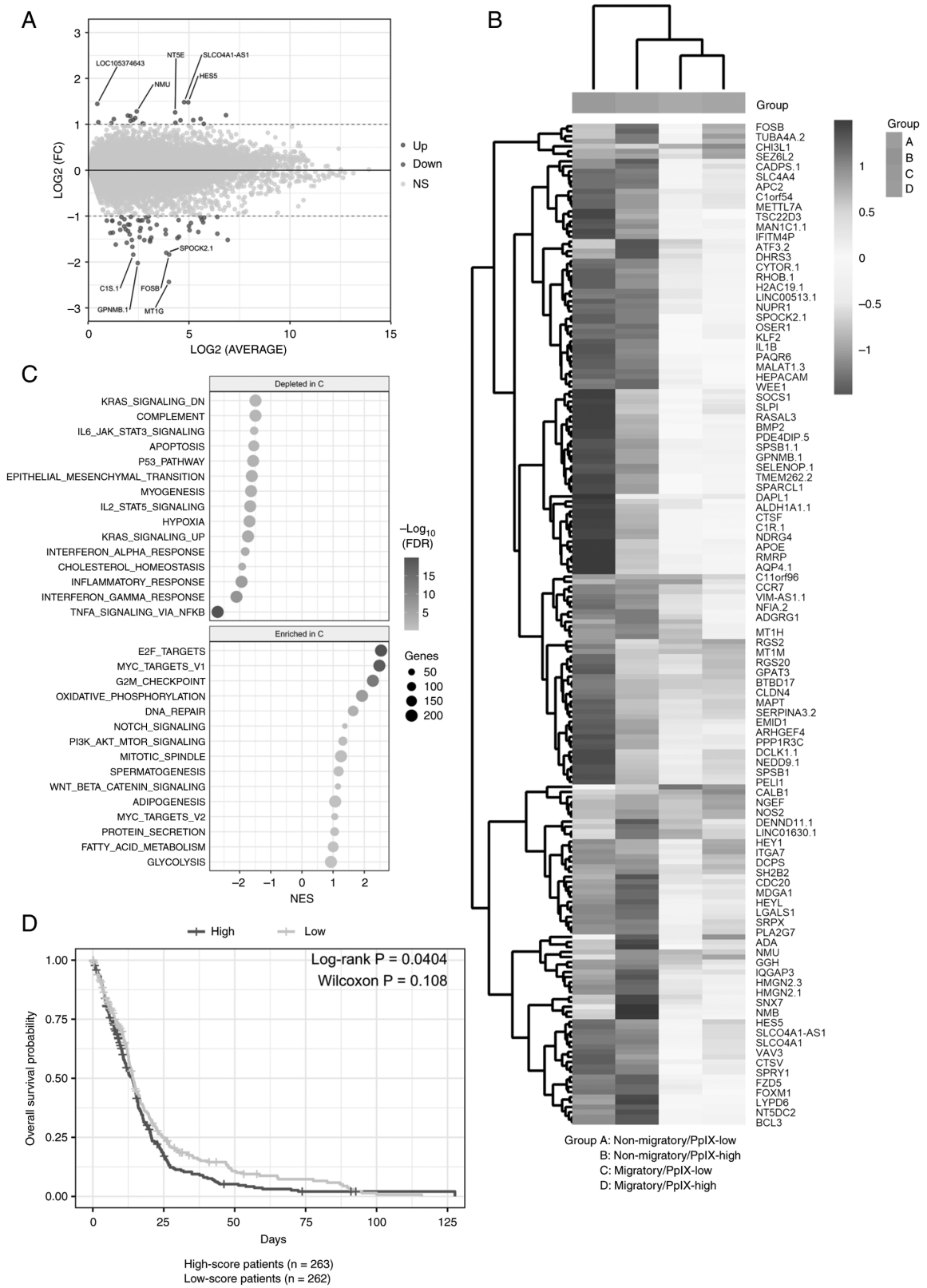

Figure 3. Transcriptomic and clinical significance of the migratory PpIX-low phenotype. (A) MA plot illustrating differential gene expression among the four subpopulations (non-migratory/PpIX-low, non-migratory/PpIX-high, migratory/PpIX-low, and migratory/PpIX-high) derived from the recurrent GBM line PDM123. Genes upregulated (>2-fold) in migratory PpIX-low cells are shown in red, downregulated (<0.5-fold) in blue. The top five genes by $|\log_2 FC|$ are annotated. (B) Heatmap of the top 200 differentially expressed genes ranked by $|\log_2 FC|$ across the four subpopulations (Group A: non-migratory/PpIX-low, B: non-migratory/PpIX-high, C: migratory/PpIX-low, and D: migratory/PpIX-high). Migratory/PpIX-low (Group C) cells showed a global downregulation pattern compared with the others. The colour scale represents z-score normalised expression. (C) Gene set enrichment analysis (GSEA) (31) dot plot summarizing the top 15 enriched pathways ranked by NES. Up- and down-regulated pathways are displayed in the lower and upper panels, respectively. Dot color indicates adjusted P-value (FDR), and dot size corresponds to gene count. Full results for the top 25 upregulated and downregulated pathways are provided in Table SI. (D) Kaplan-Meier survival analysis of 525 patients with GBM in The Cancer Genome Atlas cohort stratified by the migratory PpIX-low gene signature score. High-score patients (n=263) exhibited significantly shorter overall survival than low-score ones (n=262) (P<0.05, log-rank test). NES, normalized enrichment score; GBM, glioblastoma; 5-ALA, 5-aminolevulinic acid; PpIX, protoporphyrin IX.

genes included SLCO4A1-AS1, HES5, LOC105374643, NMU, and NT5E (CD73), whereas the most strongly downregulated genes were MT1G, GPNMB.1, C1S.1, FOSB, and SPOCK2.1 (Fig. 3A and B). These gene expression patterns suggest a coordinated shift toward a proliferative, stress-resistant, and metabolically adaptive phenotype. For instance, HES5, a Notch-pathway effector, and NT5E, an ecto-5'-nucleotidase that generates adenosine and suppresses immune activation, both contribute to stem-like persistence and microenvironmental tolerance. NMU encodes neuromedin U, a neuropeptide known to enhance GBM motility and angiogenic signaling, whereas SLCO4A1-AS1 is an antisense RNA associated with hypoxia-driven drug transport regulation. Conversely, MT1G and FOSB are oxidative stress-responsive genes typically induced by differentiation or inflammatory cues, and SPOCK2 encodes an extracellular matrix proteoglycan involved in glial maturation; their suppression further indicates an undifferentiated, high-motility cell state. GSEA of the full expression dataset provided a broader functional overview (Fig. 3C) (31), with full Hallmark enrichment results listed in Table SI. Hallmark pathways enriched among the upregulated genes included E2F_TARGETS, MYC_TARGETS_V1, G2M_CHECKPOINT, and OXIDATIVE_PHOSPHORYLATION, reflecting enhanced proliferative and metabolic activation consistent with a cycling, self-renewing phenotype. In contrast, downregulated pathways included TNFA_SIGNALING_VIA_NFKB, INTERFERON_GAMMA_RESPONSE, INFLAMMATORY_RESPONSE, and CHOLESTEROL_HOMEOSTASIS, indicating the suppression of stress-responsive and immunomodulatory transcriptional programs. This pattern suggests that migratory PpIX-low cells adopt a metabolically efficient, yet immunologically quiescent state that may permit tissue dissemination and survival under oxidative or therapeutic stress. Together with the downregulation of heme and porphyrin biosynthetic genes, these data imply that the migratory PpIX-low phenotype is sustained by a coupled transcriptional network integrating cell cycle activation, metabolic adaptation, and reduced immunogenicity, which collectively diminish 5-ALA-derived fluorescence and promote tumor persistence beyond the surgical margin. Collectively, these findings define the migratory PpIX-low state as a transcriptionally integrated mode of high-motility, metabolically adaptive, and diagnostically invisible tumor persistence.

To evaluate the clinical relevance of this program, we constructed a migratory PpIX-low gene signature comprising the top 200 differentially expressed genes (70 upregulated and 130 downregulated; Table SII) and applied it to the TCGA GBM dataset (n=525) using the GlioVis data portal (34), with the clinical survival dataset provided in Table SIII. Kaplan-Meier analysis revealed that patients with high migratory PpIX-low signature scores (n=263) exhibited a significantly shorter overall survival than those with low scores (n=262; P=0.0404, log-rank test) (Fig. 3D). Taken together, these findings establish that the migratory PpIX-low state is defined by a transcriptional program that links motility and metabolic evasion, thereby conferring both high migratory capacity and diagnostic invisibility. Its association with poor patient outcomes underscores its translational significance and suggests that therapeutic modulation of this state, by restoring porphyrin biosynthesis or sensitizing migratory cells to 5-ALA, could improve intraoperative fluorescence detection and surgical efficacy in GBM.

Discussion

In this study, we identified a transcriptional connection between cellular migratory capacity and intraoperative detectability in GBM. Across six patient-derived GBM lines, highly migratory cells consistently exhibited reduced PpIX accumulation following exposure to 5-ALA, indicating that migratory behavior and fluorescence invisibility are functionally linked rather than independent phenomena. It should be noted that the cell behavior in this study was evaluated using a two-dimensional Transwell assay without extracellular matrix coating; therefore, our findings reflect chemotactic migration rather than true extracellular matrix invasion. Within this methodological scope, the observed association provides a molecular explanation for the incomplete resection often encountered during fluorescence-guided surgery and suggests that certain GBM subpopulations may remain undetectable during PDD.

Transcriptomic profiling of phenotypically defined subpopulations revealed that the migratory PpIX-low state represents a transcriptionally integrated mode of tumor persistence that combines high migratory capacity, metabolic adaptation, and diagnostic invisibility. Upregulated genes included HES5, a Notch effector maintaining stem-like identity (35,36); NT5E (CD73), an ecto-5'-nucleotidase that generates immunosuppressive adenosine (37); NMU, a neuropeptide that promotes GBM motility and angiogenesis (38); and SLCO4A1-AS1, a hypoxia-responsive long non-coding RNA involved in drug transport regulation (39). Conversely, downregulated genes such as MT1G and FOSB, which are oxidative stress-responsive and differentiation-associated (40), and SPOCK2, an extracellular matrix proteoglycan related to glial maturation (41), suggest the loss of differentiation and acquisition of a metabolically efficient migratory phenotype.

GSEA provided a broader view of these molecular shifts, with pathways associated with E2F targets, MYC targets, the G2M checkpoint, and oxidative phosphorylation being enriched, consistent with enhanced cell cycle and metabolic activation.

In contrast, pathways linked to TNFα-NFκB signaling, interferon-γ response, inflammatory response, and cholesterol homeostasis were suppressed, indicating a transcriptional landscape favoring proliferative efficiency and immune quiescence (42). Together with the downregulation of the heme and porphyrin biosynthesis pathways, these findings suggest that migratory PpIX-low cells adopt a metabolically streamlined yet stress-tolerant state that supports migration-associated dissemination and survival under therapeutic or oxidative pressure. This state may underlie their ability to escape intraoperative detection and contribute to tumor recurrence.

Clinically, the migratory PpIX-low gene signature was associated with significantly poorer overall survival in the TCGA GBM cohort, supporting its translational relevance (43). Concordance between *in vitro* fluorescence phenotypes and patient transcriptomic data implies that the molecular determinants of 5-ALA detectability reflect clinically meaningful

tumor biology (44). Accordingly, the migratory PpIX-low signature may serve as a potential biomarker for predicting incomplete resection and recurrence risk (44), and therapeutic modulation of this state, by restoring porphyrin biosynthesis or sensitizing migratory cells to 5-ALA, could improve intraoperative tumor visualization and surgical efficacy in GBM.

This study had several limitations. Our analysis was based on six patient-derived lines and focused primarily on *in vitro* phenotypes; thus, the causal links between transcriptional programs and 5-ALA accumulation remain to be validated *in vivo*. Although we observed a consistent association between migratory capacity and reduced PpIX accumulation, alternative explanations should be considered. Although equal numbers of single cells were seeded into the upper chamber and migration was assessed within a defined time window under serum-free conditions, differences in proliferative activity could theoretically influence migration-based measurements. However, the positive correlation between migratory index and PpIX-negative fraction across independent cell lines suggests a stable phenotypic association rather than a transient growth-rate effect. Differences in cell-cycle distribution may influence porphyrin biosynthesis, because cycling cells exhibit altered metabolic demands that could affect PpIX synthesis. Furthermore, variability in 5-ALA uptake, intracellular transport, or efflux mechanisms, independent of migratory status, may contribute to the heterogeneous fluorescence intensity. Although our transcriptomic analyses support a coordinated molecular program linking motility and metabolic regulation, these alternative mechanisms cannot be excluded and warrant direct experimental validation. Future studies employing genetic manipulation and orthotopic xenograft models are necessary to determine whether altering this transcriptional network can modify tumor behavior or fluorescence responsiveness. In addition, while our Transwell system evaluated single-cell chemotactic migration, complementary models assessing collective migration dynamics (e.g., wound healing-type assays) may further refine the phenotypic characterization of GBM motility in future investigations. Despite these limitations, the present work provides a conceptual framework for understanding the molecular basis of the diagnostic invisibility associated with migratory GBM cell states and establishes a foundation for translational approaches to improve fluorescence-guided resection.

In summary, this study revealed a transcriptional network linking high migratory capacity with reduced 5-ALA-based fluorescence detectability in GBM.

Acknowledgements

We thank Ms. Marika Nodera (Institute of Science Tokyo, Tokyo, Japan) for her technical assistance, Dr. Yoshitaka Murota (Institute of Science Tokyo, Tokyo, Japan) for his valuable discussions, and Professor Genki Kanda (Institute of Science Tokyo, Tokyo, Japan) for providing the research environment for this work.

Funding

This work was supported by the Japan Society for the Promotion of Science KAKENHI for Scientific Research (grant no. 24K10354) and JST CREST (grant no. JPMJCR2551). Additional support was provided by the Medical Research Center Initiative for High-Depth Omics, Nanken-Kyoten (grant nos. 2023-kokusai 01, 2024-kokunai 11, and 2025-kokunai 45), and Multilayered Stress Diseases (grant no. JPMXP1323015483), Science Tokyo.

Availability of data and materials

The data generated in the present study may be requested from the corresponding author. The microarray data generated in the present study have been deposited in the Gene Expression Omnibus (GEO) under accession number GSE320501 and are available at https://www.ncbi.nlm.nih.gov/geo/query/acc.cgi?acc=GSE320501.

Authors' contributions

KT conceived and designed the study, curated and analyzed the data, and secured funding. TZ contributed to the investigation by performing the experiments. WL contributed to data analysis and interpretation. KT and TZ developed the methodology. IS, TH and TK contributed to acquisition of clinical samples and interpretation of data. SO contributed to experimental design and data interpretation. KT and TT supervised the study, and TT contributed to study design and data interpretation. KT validated the experiments, generated the figures, and wrote the original draft. All authors contributed to reviewing and editing the manuscript. All authors have read and approved the final manuscript. KT and TT confirm the authenticity of all the raw data.

Ethics approval and consent to participate

All procedures involving human specimens were approved by the Human Ethics Review Boards of the Kumamoto University School of Medicine (approval no. 231) and Kitasato University School of Medicine (approval no. B20-088) and conducted in accordance with the Declaration of Helsinki, with written informed consent obtained from all patients. All experiments involving recombinant DNA were approved by the Recombinant DNA Safety Committee of the Institute of Science Tokyo, Japan (approval nos. G2018-083C, G2023-051C, G2025-005A) and conducted in compliance with national regulations.

Patient consent for publication

Not applicable.

Competing interests

The authors declare that they have no competing interests.

References

1. Pouyan A, Ghorbanlo M, Eslami M, Jahanshahi M, Ziaei E, Salami A, Mokhtari K, Shahpasand K, Farahani N, Meybodi TE, *et al*: Glioblastoma multiforme: Insights into pathogenesis, key signaling pathways, and therapeutic strategies. Mol Cancer 24: 58, 2025.

2. Ostrom QT, Patil N, Cioffi G, Waite K, Kruchko C and Barnholtz-Sloan JS: CBTRUS statistical report: Primary brain and other central nervous system tumors diagnosed in the United States in 2013-2017. Neuro Oncol 22 (12 Suppl 2): iv1-iv96, 2020.
3. Wang L, Liang B, Li YI, Liu X, Huang J and Li YM: What is the advance of extent of resection in glioblastoma surgical treatment-a systematic review. Chin Neurosurg J 5: 2, 2019.
4. Roh TH and Kim SH: Supramaximal resection for glioblastoma: Redefining the extent of resection criteria and its impact on survival. Brain Tumor Res Treat 11: 166-172, 2023.
5. Kow CY, Kim BJH, Park TIH, Chen JCC, Vong CK, Kim JY, Shim V, Dragunow M and Heppner P: Extent of resection affects prognosis for patients with glioblastoma in non-eloquent regions. J Clin Neurosci 80: 242-249, 2020.
6. Stummer W, Reulen HJ, Meinel T, Pichlmeier U, Schumacher W, Tonn JC, Rohde V, Oppel F, Turowski B, Woiciechowsky C, *et al*: Extent of resection and survival in glioblastoma multiforme: Identification of and adjustment for bias. Neurosurgery 62: 564-576, 2008.
7. Stendel R: Extent of resection and survival in glioblastoma multiforme: Identification of and adjustment for bias. Neurosurgery 64: E1206, 2009.
8. Casas A: Clinical uses of 5-aminolaevulinic acid in photodynamic treatment and photodetection of cancer: A review. Cancer Lett 490: 165-173, 2020.
9. Maragkos GA, Schüpper AJ, Lakomkin N, Sideras P, Price G, Baron R, Hamilton T, Haider S, Lee IY, Hadjipanayis CG and Robin AM: Fluorescence-guided high-grade glioma surgery more than four hours after 5-aminolevulinic acid administration. Front Neurol 12: 644804, 2021.
10. Hadjipanayis CG and Stummer W: 5-ALA and FDA approval for glioma surgery. J Neurooncol 141: 479-486, 2019.
11. Stummer W, Novotny A, Stepp H, Goetz C, Bise K and Reulen HJ: Fluorescence-guided resection of glioblastoma multiforme by using 5-aminolevulinic acid-induced porphyrins: A prospective study in 52 consecutive patients. J Neurosurg 93: 1003-1013, 2000.
12. Mazurek M, Szczepanek D, Orzyłowska A and Rola R: Analysis of factors affecting 5-ALA fluorescence intensity in visualizing glial tumor cells-literature review. Int J Mol Sci 23: 926, 2022.
13. Stummer W, Pichlmeier U, Meinel T, Wiestler OD, Zanella F and Reulen HJ; ALA-Glioma Study Group: Fluorescence-guided surgery with 5-aminolevulinic acid for resection of malignant glioma: A randomised controlled multicentre phase III trial. Lancet Oncol 7: 392-401, 2006.
14. Stummer W, Tonn JC, Goetz C, Ullrich W, Stepp H, Bink A, Pietsch T and Pichlmeier U: 5-Aminolevulinic acid-derived tumor fluorescence: The diagnostic accuracy of visible fluorescence qualities as corroborated by spectrometry and histology and postoperative imaging. Neurosurgery 74: 310-320, 2014.
15. Roberts DW, Valdés PA, Harris BT, Fontaine KM, Hartov A, Fan X, Ji S, Lollis SS, Pogue BW, Leblond F, *et al*: Coregistered fluorescence-enhanced tumor resection of malignant glioma: Relationships between ð-aminolevulinic acid-induced protoporphyrin IX fluorescence, magnetic resonance imaging enhancement, and neuropathological parameters. Clinical article. J Neurosurg 114: 595-603, 2011.
16. Lau D, Hervey-Jumper SL, Chang S, Molinaro AM, McDermott MW, Phillips JJ and Berger MS: A prospective phase II clinical trial of 5-aminolevulinic acid to assess the correlation of intraoperative fluorescence intensity and degree of histologic cellularity during resection of high-grade gliomas. J Neurosurg 124: 1300-1309, 2016.
17. Idoate MA, Díez Valle R, Echeveste J and Tejada S: Pathological characterization of the glioblastoma border as shown during surgery using 5-aminolevulinic acid-induced fluorescence. Neuropathology 31: 575-582, 2011.
18. Omoto K, Matsuda R, Nakai Y, Tatsumi Y, Nakazawa T, Tanaka Y, Shida Y, Murakami T, Nishimura F, Nakagawa I, *et al*: Expression of peptide transporter 1 has a positive correlation in protoporphyrin IX accumulation induced by 5-aminolevulinic acid with photodynamic detection of non-small cell lung cancer and metastatic brain tumor specimens originating from non-small cell lung cancer. Photodiagnosis Photodyn Ther 25: 309-316, 2019.
19. Hagiya Y, Fukuhara H, Matsumoto K, Endo Y, Nakajima M, Tanaka T, Okura I, Kurabayashi A, Furihata M, Inoue K and Ogura SI: Expression levels of PEPT1 and ABCG2 play key roles in 5-aminolevulinic acid (ALA)-induced tumor-specific protoporphyrin IX (PpIX) accumulation in bladder cancer. Photodiagnosis Photodyn Ther 10: 288-295, 2013.
20. Hou C, Yamaguchi S, Ishi Y, Terasaka S, Kobayashi H, Motegi H, Hatanaka KC and Houkin K: Identification of PEPT2 as an important candidate molecule in 5-ALA-mediated fluorescence-guided surgery in WHO grade II/III gliomas. J Neurooncol 143: 197-206, 2019.
21. Morita M, Tanaka H, Kumamoto Y, Nakamura A, Harada Y, Ogata T, Sakaguchi K, Taguchi T and Takamatsu T: Fluorescence-based discrimination of breast cancer cells by direct exposure to 5-aminolevulinic acid. Cancer Med 8: 5524-5533, 2019.
22. Wang W, Tabu K, Hagiya Y, Sugiyama Y, Kokubu Y, Murota Y, Ogura SI and Taga T: Enhancement of 5-aminolevulinic acid-based fluorescence detection of side population-defined glioma stem cells by iron chelation. Sci Rep 7: 42070, 2017.
23. D'Amico AG, Maugeri G, Vanella L, Consoli V, Sorrenti V, Bruno F, Federico C, Fallica AN, Pittalà V and D'Agata V: Novel acetamide-based HO-1 inhibitor counteracts glioblastoma progression by interfering with the hypoxic-angiogenic pathway. Int J Mol Sci 25: 5389, 2024.
24. Virtuoso A, D'Amico G, Scalia F, De Luca C, Papa M, Maugeri G, D'Agata V, Caruso Bavisotto C and D'Amico AG: The interplay between glioblastoma cells and tumor microenvironment: New perspectives for early diagnosis and targeted cancer therapy. Brain Sci 14: 331, 2024.
25. D'Amico AG, Caruso Bavisotto C and Virtuoso A: Identification of molecular targets and anti-cancer agents in GBM: New perspectives for cancer therapy. Brain Sci 13: 1078, 2023.
26. D'Amico AG, Maugeri G, Magrì B, Giunta S, Saccone S, Federico C, Pricoco E, Broggi G, Caltabiano R, Musumeci G, *et al*: Modulatory activity of ADNP on the hypoxia-induced angiogenic process in glioblastoma. Int J Oncol 62: 14, 2023.
27. Ihata T, Nonoguchi N, Fujishiro T, Omura N, Kawabata S, Kajimoto Y and Wanibuchi M: The effect of hypoxia on photodynamic therapy with 5-aminolevulinic acid in malignant gliomas. Photodiagnosis Photodyn Ther 40: 103056, 2022.
28. Maugeri G, D'Amico AG, Saccone S, Federico C, Rasà DM, Caltabiano R, Broggi G, Giunta S, Musumeci G and D'Agata V: Effect of PACAP on hypoxia-induced angiogenesis and epithelial-mesenchymal transition in glioblastoma. Biomedicines 9: 965, 2021.
29. Kostron H: Photodynamic diagnosis and therapy and the brain. Methods Mol Biol 635: 261-280, 2010.
30. Park J, Oh SJ, Shim JK, Ji YB, Moon JH, Kim EH, Huh YM, Suh JS, Chang JH, Lee SJ and Kang SG: C5α secreted by tumor mesenchymal stem-like cells mediates resistance to 5-aminolevulinic acid-based photodynamic therapy against glioblastoma tumorspheres. J Cancer Res Clin Oncol 149: 4391-4402, 2023.
31. Subramanian A, Tamayo P, Mootha VK, Mukherjee S, Ebert BL, Gillette MA, Paulovich A, Pomeroy SL, Golub TR, Lander ES and Mesirov JP: Gene set enrichment analysis: A knowledge-based approach for interpreting genome-wide expression profiles. Proc Natl Acad Sci USA 102: 15545-15550, 2005.
32. Korotkevich G, Sukhov V, Budin N, Shpak B, Artyomov MN and Sergushichev A: Fast gene set enrichment analysis. bioRxiv: 060012, 2021.
33. Liberzon A, Birger C, Thorvaldsdóttir H, Ghandi M, Mesirov JP and Tamayo P: The molecular signatures database (MSigDB) hallmark gene set collection. Cell Syst 1: 417-425, 2015.
34. Bowman RL, Wang Q, Carro A, Verhaak RG and Squatrito M: GlioVis data portal for visualization and analysis of brain tumor expression datasets. Neuro Oncol 19: 139-141, 2017.
35. Giachino C, Boulay JL, Ivanek R, Alvarado A, Tostado C, Lugert S, Tchorz J, Coban M, Mariani L, Bettler B, *et al*: A tumor suppressor function for notch signaling in forebrain tumor subtypes. Cancer Cell 28: 730-742, 2015.
36. Chung S and Kim C: Comparative analysis of transcription factors TWIST2, GATA3, and HES5 in glioblastoma multiforme: Evaluating biomarker potential and therapeutic targets using in silico methods. J Korean Neurosurg Soc 68: 202-212, 2025.
37. Wang M, Jia J, Cui Y, Peng Y and Jiang Y: CD73-positive extracellular vesicles promote glioblastoma immunosuppression by inhibiting T-cell clonal expansion. Cell Death Dis 12: 1065, 2021.
38. Przygodzka P, Soboska K, Sochacka E and Boncela J: Erratum: Neuromedin U: A small peptide in the big world of cancer. Cancers 2019, 11, 1312. Cancers (Basel) 12: 251, 2020.

39. Wu Y, Li F, Yang C, Zhang X, Xue Z, Sun Y, Lin X, Liu X, Zhao Z, Huang B, *et al*: Super-enhancer-driven SLCO4A1-AS1 is a new biomarker and a promising therapeutic target in glioblastoma. Sci Rep 15: 954, 2025.
40. Qi M, Sun LA, Zheng LR, Zhang J, Han YL, Wu F, Zhao J, Niu WH, Fei MX, Jiang XC and Zhou ML: Expression and potential role of FOSB in glioma. Front Mol Neurosci 15: 972615, 2022.
41. Xiao M, Xue J and Jin E: SPOCK: Master regulator of malignant tumors (review). Mol Med Rep 30: 231, 2024.
42. Mao H, Zhao X and Sun SC: NF-κB in inflammation and cancer. Cell Mol Immunol 22: 811-839, 2025.
43. Ceccarelli M, Barthel FP, Malta TM, Sabedot TS, Salama SR, Murray BA, Morozova O, Newton Y, Radenbaugh A, Pagnotta SM, *et al*: Molecular profiling reveals biologically discrete subsets and pathways of progression in diffuse glioma. Cell 164: 550-563, 2016.
44. Widhalm G, Olson J, Weller J, Bravo J, Han SJ, Phillips J, Hervey-Jumper SL, Chang SM, Roberts DW and Berger MS: The value of visible 5-ALA fluorescence and quantitative protoporphyrin IX analysis for improved surgery of suspected low-grade gliomas. J Neurosurg 133: 79-88, 2019.